TIME-RESOLVED INFRARED RADIOMETRY (TRIR) FOR CHARACTERIZATION OF IMPACT DAMAGE IN COMPOSITE MATERIALS

J. W. Maclachlan Spicer, W. D. Kerns, L. C. Aamodt, and J. C. Murphy

Center for NDE & Applied Physics Laboratory
The Johns Hopkins University
Johns Hopkins Road, Laurel, MD 20723-6099, USA

INTRODUCTION

A quantitative thermographic NDE technique for the characterization of impact damage in composite materials is under development along with supporting theoretical analysis. We have previously shown that the technique of time-resolved infrared radiometry (TRIR) is an effective method for quantitatively detecting coating thickness variations and for characterizing the degree of coating disbonding in terms of equivalent air gaps [1,2]. Here we extend the TRIR technique to the study of composite systems by applying the results of a multilayer analytical model [3]. Experimental results in both simple and hybrid composite systems are discussed. The depth and lateral extent of interlaminar separation in composites subjected to impact loading is presented and the use of lateral heat flow techniques to image defect structures is examined.

TIME-RESOLVED INFRARED RADIOMETRY TECHNIQUE

The TRIR technique differs from other pulsed thermography techniques in that the surface temperature of the specimen is monitored as a function of time during the application of a step heating pulse to the sample. Full-field images with temporal resolution faster than video frame rates are acquired by disabling the vertical galvanometer in the infrared camera and scanning the heating source across the sample. TRIR X-Y images at different time intervals after the onset of the heating pulse reveal spatial variations in the temperature response across the sample. It is necessary, however, to analyze the temperature-time response as a function of position on the sample to provide thermal transit times indicating the depth of defects and the shape of the curve indicating the thermal resistance of the defect.

A summary of the range of TRIR temperature versus square root time (T_S-$t^{1/2}$) linescans obtained for a series of specimen configurations and experimental situations is given in Fig. 1. Curves A and B indicate the temperature response obtained when a thermally insulating defect is located at a certain depth in a thermally conductive specimen. The surface temperature of the specimen rises as the square root of time (indicated by the dashed line in the figure) until the thermal transit time is reached. This time is given by $0.38\ L^2/\alpha$ where L is the depth of the defect and α is the specimen thermal diffusivity. After the thermal transit time the slope of the curve increases due to the presence of the thermally-insulating defect. Should the subsurface structure be more thermally conductive than the surface layer, the response shown in Curve D is obtained where the slope of the curve decreases at the thermal transit time.

Review of Progress in Quantitative Nondestructive Evaluation, Vol. 11
Edited by D.O. Thompson and D.E. Chimenti, Plenum Press, New York, 1992

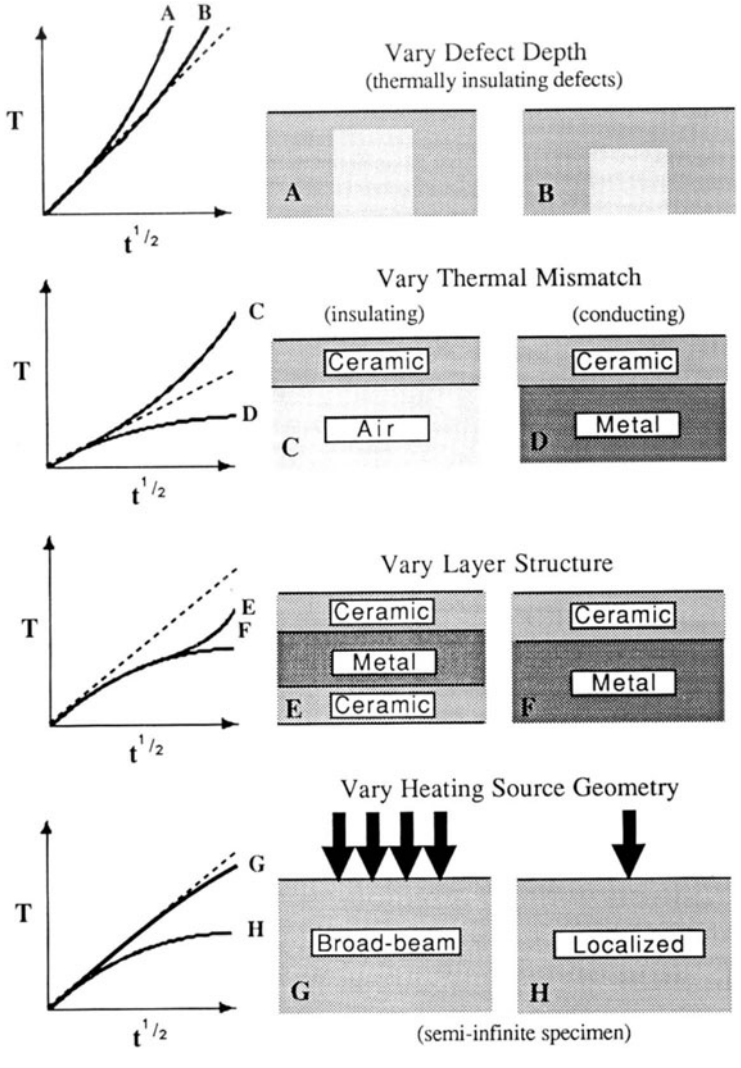

Figure 1 Summary of typical TRIR T_S-$t^{1/2}$ linescans obtained for a series of specimen configurations and experimental situations.

The TRIR technique can be applied to multilayered samples as indicated by Curve E where the presence of a thermally insulating layer is detected beneath another thermally insulating layer and a thermally conductive layer. The capability for multilayer analysis is heavily dependent on the relative thermal properties of the different layers [3] but our initial observations show that the TRIR technique has great promise for imaging defects in multilayer systems such as composites.

The final pair of curves in Fig. 1 indicate the role of the geometry of the heating beam in determining the TRIR response. While one-dimensional models are applicable for broad area heating of the sample (Curve G), three-dimensional models are required to describe the lateral heat flow occurring in the specimen when the heating beam has a finite extent [4]. It is possible to obtain simultaneous information about through-thickness and lateral thermal diffusivities if the geometry of the heating beam is chosen appropriately. In addition, the presence of vertical defects can be detected through their influence on the lateral heat flow.

The experimental system used to conduct these measurements consists of an infrared scanner (Mikron 6T61) to monitor the specimen surface temperature as a function of time, synchronizing electronics and an acousto-optic modulator to gate the heating beam from an argon ion laser (Coherent Innova 90-5) at a fixed time with respect to the frame rate of the scanner, and a positioning system (Aerotech Unidex XII) to translate the specimen with respect to the heating source. Operation of the infrared scanner, synchronizing electronics and positioning system is all under the control of a microcomputer (Macintosh II) over the IEEE-488 bus.

DETECTION OF SUBSURFACE HOLES IN CARBON/CARBON COMPOSITE

Initial TRIR tests were made on a carbon/carbon composite specimen which had a series of small, flat bottomed holes drilled to produce a defect of continually increasing depth as shown in Fig. 2.

A TRIR X-Y scan was performed over the region indicated in Fig. 2 and the results of this scan are shown in Fig. 3(a). A number of reference points in Fig. 2 indicating different locations on the specimen with respect to the defects are also shown on the image in Fig. 3(a).

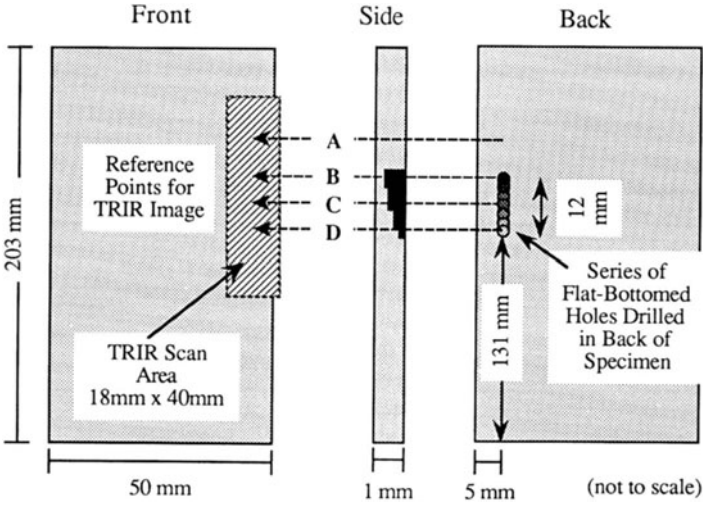

Figure 2 Diagram of carbon/carbon composite specimen with flat-bottomed holes drilled from the back face. The TRIR scan region on the front face is shown.

Note that the image representation for this data for the purposes of publication consists of a grey scale map with contour lines superimposed on the image. Actual image analysis was conducted with the aid of false-color maps which greatly enhanced the visibility of the defects. This data was acquired using a line heating source with a Gaussian profile and with extent approximately 2 mm x 18 mm. This line source was stepped across the sample for 400 steps with a step size of 100 μm to give a total vertical scan distance of 40 mm. A heating pulse length of 1 second was used and the range of the temperature rise for the data shown in Fig. 3(a) is about 12 °C.

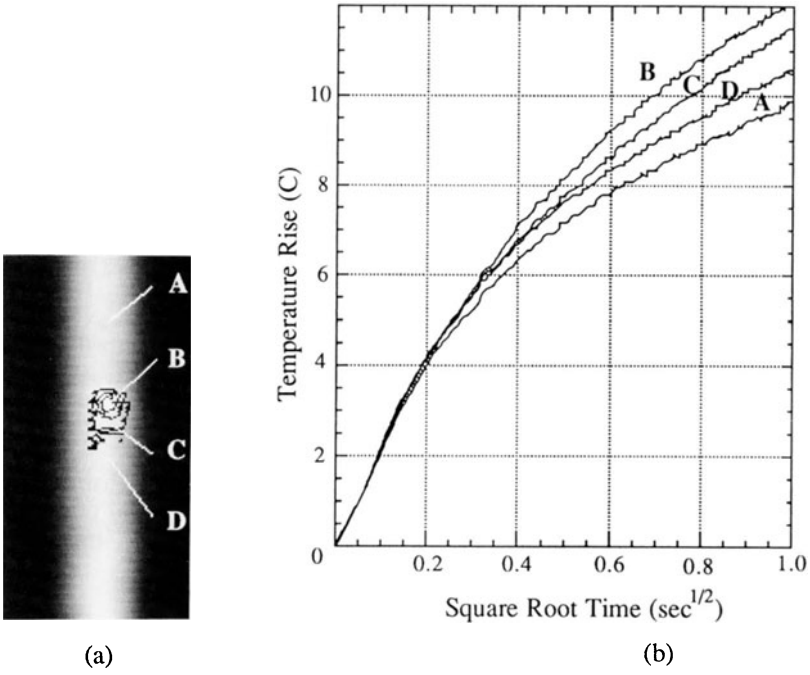

(a) (b)

Figure 3 (a) TRIR X-Y image for area on back face of hybrid composite shown in Fig. x.
(b) TRIR T_S-$t^{1/2}$ linescans for the locations marked on the TRIR image.

TRIR T_S-$t^{1/2}$ linescans for the 4 locations identified on the image are given in Fig. 3(b). Note that none of these linescans shows the classic response expected for the presence of insulating defects of increasing depth (see Curves A and B in Fig. 1) but instead show a curving over behavior due to the presence of a significant amount lateral heat flow in the highly conductive carbon/carbon composite (see Curve H in Fig. 1). There is, however, a variation between these curves, even in the presence of significant lateral heat flow. As is expected [4], Location B with the shallowest defect shows a greater temperature excursion than Locations C and D which have deeper defects. All three of these responses lie above that obtained for Location A where there were no defects. These results show that subsurface defects can be detected and distinguished on the basis of their depth in carbon/carbon composites using the TRIR technique.

The next series of TRIR experiments were conducted in a more complicated hybrid composite shown in Fig. 4 which consisted of a multilayer graphite/epoxy layup with face sheets of single ply E-glass/epoxy composite. This specimen had been subjected to projectile loading producing a localized hole in the front of the sample and more extensive damage on the back face. Some preliminary TRIR measurements were made on the E-glass epoxy material alone in order to determine the thermal diffusivity of this material. A specimen of thickness 1.68 mm (this is thicker than that used in the hybrid composite specimen) was first tested free-standing in air and then tested with an aluminum heat sink as a backing. The resulting T_S-$t^{1/2}$ linescans are shown in Fig. 5 and show the expected response (see Curves C and D in Fig. 1) with a thermal transit time for the specimen of 1.35 $sec^{1/2}$ or 1.82 sec. The dashed line represents the response which would be obtained for a thermally-thick specimen and is used as a reference curve. The thermal diffusivity for the E-glass/epoxy composite is calculated to be 0.00589 cm^2/sec. This then indicates that the thermal transit time for the 0.4 mm layer used in the hybrid composite should be about 0.103 sec or 0.32 $sec^{1/2}$.

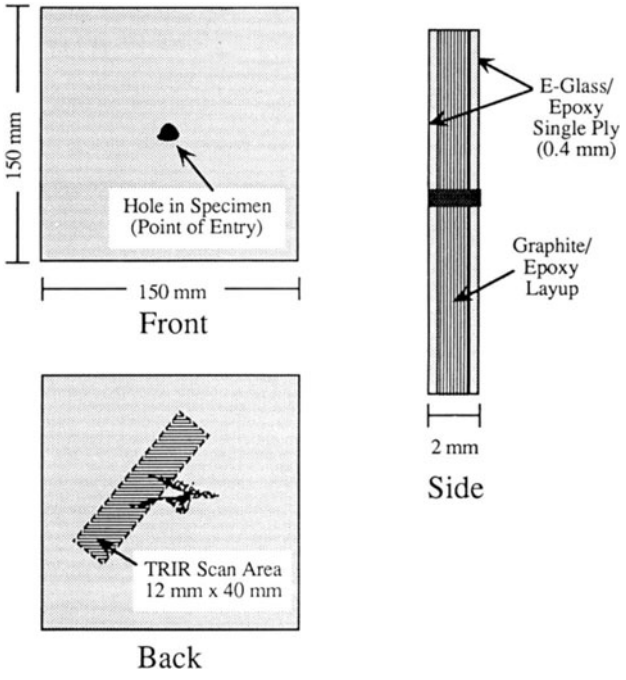

Figure 4 Diagram of hybrid composite specimen subjected to impact testing showing TRIR scan region on the back face.

A TRIR X-Y image for the hybrid composite was performed over the region indicated in Fig. 4 again using a line heating source with a Gaussian profile and with an extent of approximately 2 mm x 18 mm. This data is shown in Fig. 6(a) using the same grey scale-contour representation as in Fig. 3. The total vertical scan distance was 80 mm with 400 steps of 200 μm step size. A 5 second heating pulse length was used and the range of the temperature rise for the data was about 9 °C.

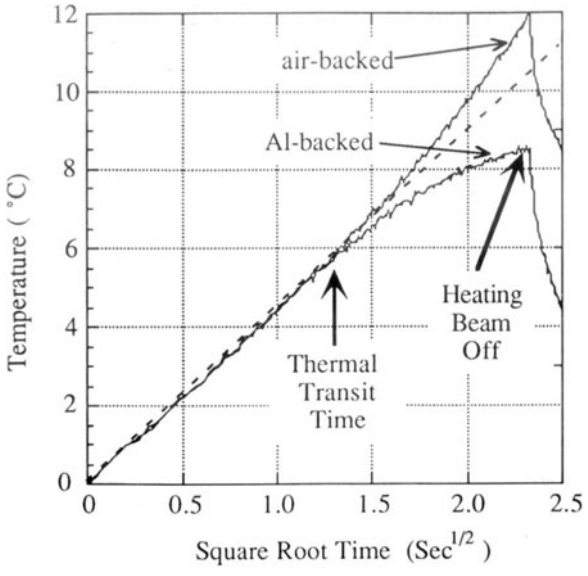

Figure 5 TRIR T_s-$t^{1/2}$ linescans for specimen of E-glass/epoxy composite in air (top curve) and heat sunk to aluminum block (lower curve).

The T_s-$t^{1/2}$ linescans for the positions indicated on the image are given in Fig. 6(b). Note that all of the curves follow the square root of time until about 0.3 $sec^{1/2}$ which is the expected thermal transit time for the E-glass/epoxy layer. At this time the data for Location A which is well-removed from the damaged area in the specimen shows a slope decrease as is expected for a well-bonded region of the specimen. The curves for the other locations where damage has occurred all show a slope increase at this location. The shape of these curves does vary, however, and at present we interpret this as resulting from different degrees of delamination of the E-glass/epoxy layer from the graphite-epoxy layup. Similar results have been observed in TRIR measurements on coating systems [3].

A second series of TRIR X-Y images were performed on the hybrid composite specimen using a Gaussian heating beam of diameter 12 mm. The comparison between the TRIR X-Y images acquired with the Gaussian and line heating sources is given in Fig. 7. Note that while the overall shape of the damage region is similar in the two images, there is far more resolution of independent structures in the image using the line source. Since the dimension of the line source in the Y direction is only about 2 mm, it is expected that significant lateral heat flow occurs in this case. The detection of discrete structures in these images may indicate the presence of vertical defects which are detected by the lateral heat flow. Further analysis of these results is underway.

CONCLUSIONS

The results presented here demonstrate that the TRIR technique is appropriate for impact damage assessment in composite materials. The depth of damage can be determined through analysis of the thermal transit times and the TRIR results show sensitivity to the degree of delamination. It is also shown that lateral heat flow effects are important for spatial localization of damage and three-dimensional modelling of heat flow at the level of the ply structure of the composite is in progress to further explain these results.

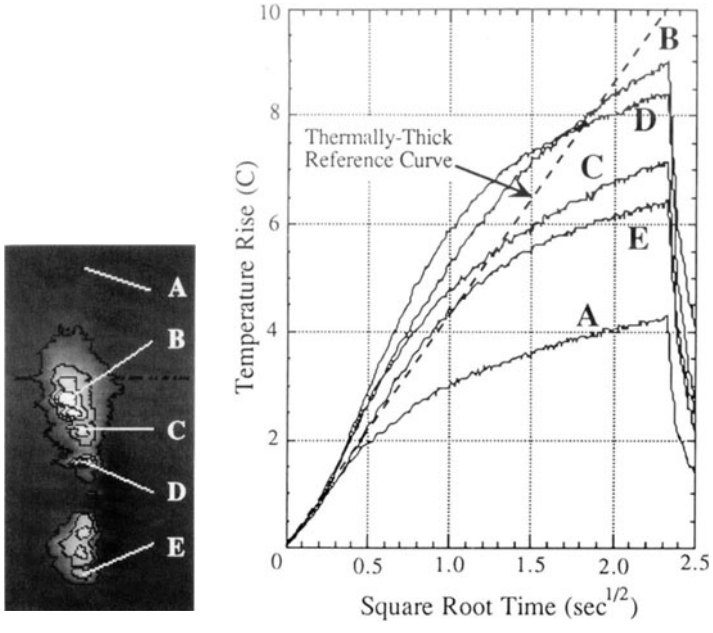

Figure 6 (a) TRIR X-Y image for area on back face of hybrid composite shown in Fig. 4. (b) TRIR T_S-$t^{1/2}$ linescans for the locations marked on the TRIR image.

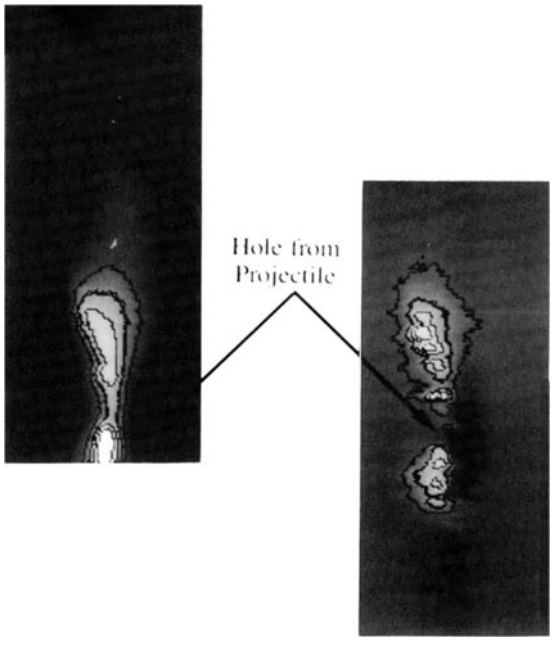

Figure 7 Comparison of TRIR X-Y images of hybrid composite specimen for Gaussian (left) and line source (right) heating beam geometries.

ACKNOWLEDGEMENTS

This work was supported by the Air Force Program in QNDE through Iowa State University and by the U.S. Department of the navy under Contract N00038-89-C-5301.

REFERENCES

1. J.W. Maclachlan Spicer, W.D. Kerns, L.C. Aamodt and J.C. Murphy, J. Nondestructr. Eval. 8, No. 2, 107-120 (1989).
2. J.W. Maclachlan Spicer, W.D. Kerns, L.C. Aamodt and J.C. Murphy, in Review of Progress in Quantitative NDE, edited by D.O. Thompson and D.E. Chimenti (Plenum Press, New York, 1991) Vol. 10, pp. 1193-1200.
3. L.C. Aamodt, J.W. Maclachlan Spicer and J.C. Murphy, J. Appl. Phys. 68, No. 12, 6087-6098 (1990).
4. L.C. Aamodt, J.W. Maclachlan Spicer and J.C. Murphy, in Photoacoustic and Photothermal Phenomena II, edited by J.C. Murphy, J.W. Maclachlan Spicer, L.Aamodt and B.S.H. Royce (Springer-Verlag Berlin, Heidelberg 1990) pp. 59-63.